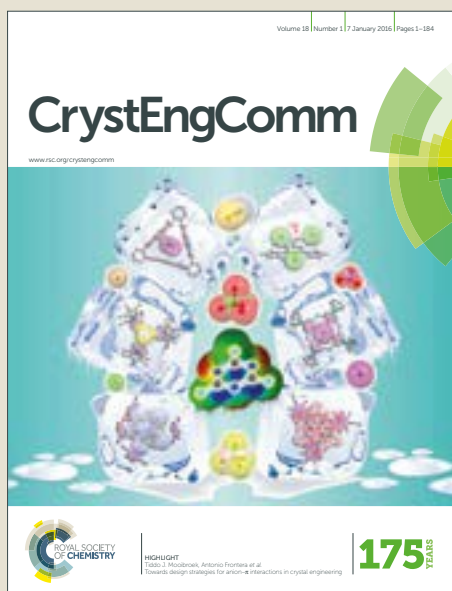


CrystEngComm

Accepted Manuscript



This article can be cited before page numbers have been issued, to do this please use: M. Enamullah, V. Vasylieva, M. A. Quddus, M. K. Islam, S. Höfert and C. Janiak, *CrystEngComm*, 2018, DOI: 10.1039/C8CE00839F.

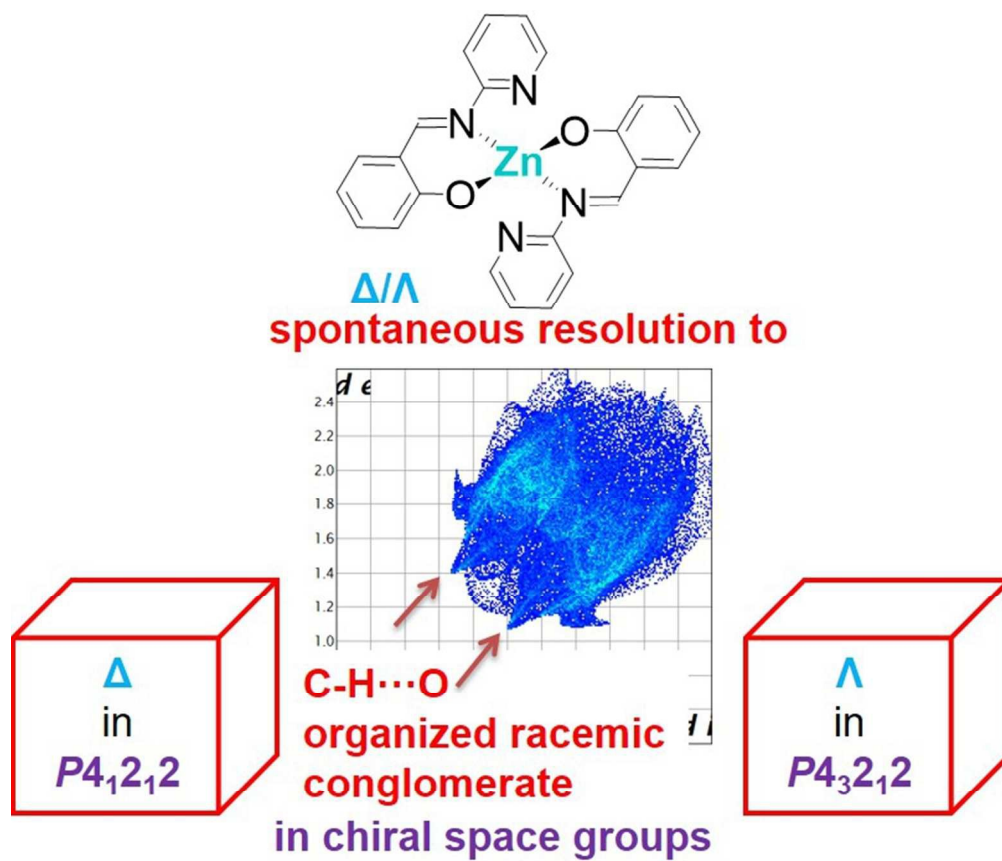


This is an Accepted Manuscript, which has been through the Royal Society of Chemistry peer review process and has been accepted for publication.

Accepted Manuscripts are published online shortly after acceptance, before technical editing, formatting and proof reading. Using this free service, authors can make their results available to the community, in citable form, before we publish the edited article. We will replace this Accepted Manuscript with the edited and formatted Advance Article as soon as it is available.

You can find more information about Accepted Manuscripts in the [author guidelines](#).

Please note that technical editing may introduce minor changes to the text and/or graphics, which may alter content. The journal's standard [Terms & Conditions](#) and the ethical guidelines, outlined in our [author and reviewer resource centre](#), still apply. In no event shall the Royal Society of Chemistry be held responsible for any errors or omissions in this Accepted Manuscript or any consequences arising from the use of any information it contains.



136x119mm (150 x 150 DPI)

Cite this: DOI: XX.XXXX/x0xx00000x

www.rsc.org/xxxxxx

PAPER

Spontaneous resolution of a Δ/Λ -chiral-at-metal pseudo-tetrahedral Schiff-base zinc complex to a racemic conglomerate with C–H \cdots O organized 4₁- and 4₃-helices†

Mohammed Enamullah,^{a,*} Vera Vasylyeva,^b Mohammad Abdul Quddus,^a Mohammad Khairul Islam,^a Simon-Patrick Höfert,^b and Christoph Janiak^{b,*}

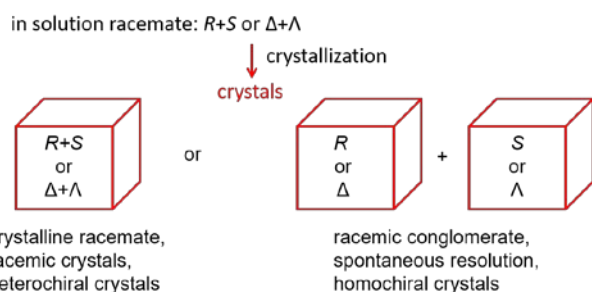
Received (in XXX, XXX) Xth XXXXXXXXX 20XX, Accepted Xth XXXXXXXXX 20XX

DOI: 10.1039/b000000x

The Schiff-base ligand, *N*-2-(pyridyl)salicylaldimine (HL) reacts with zinc(II) acetate or nitrate to give the enantiomorphous chiral-at-metal compound Δ/Λ -bis[*N*-2-(pyridyl)salicylaldiminato- κ^2 N,O]zinc(II), [Zn(L)₂] (**1**), which crystallizes as a racemic conglomerate *via* spontaneous resolution. Two deprotonated N,O-chelate ligands form a pseudo-tetrahedral N₂O₂-coordination sphere with a Δ/Λ -configured zinc atom. The Δ - and Λ -configured molecular complexes in **1** assemble in *P* (right)- and *M* (left)-handed 4₁- and 4₃-helical chains in the chiral space groups *P*4₁2₁2 and *P*4₃2₁2, respectively, through weak C–H \cdots O hydrogen bonding between neighbouring molecules along the chain axis. Only molecules of the same Δ - or Λ -configuration are combined into a helical chain and only the chains of the same *P*- or *M*-handedness are combined to form homochiral crystals. The supramolecular packing from the analyses of intermolecular interactions with the Hirshfeld surface features C–H \cdots O bonding as the most apparent significant contributions. This is a rare example of solely weak C–H \cdots O hydrogen bonding interactions that leads to spontaneous resolution to a racemic conglomerate. The case also supports the notion of less repulsive packing interactions between homochiral molecules because of spin polarization. Optimized structures and excited state properties by DFT/TD-DFT calculations are comparable to the experimental results.

Introduction

When a racemic compound crystallizes it can form either a crystalline racemate containing both enantiomers in the same crystal in equal amounts (heterochiral crystals), or a racemic conglomerate, that is an equimolar mixture of separate crystals where each one contains only one of the two enantiomers (homochiral crystals) (Scheme 1).^{1,2,3} The later phenomenon is termed as spontaneous resolution.



Scheme 1 Schematic presentation of the possible differences in crystal formation from a racemic solution mixture. *R*, *S* are the designations (devised by Cahn, Ingold and Prelog) of absolute configuration at four-coordinate and six-coordinate stereogenic centers. Δ (Delta), Λ (Lambda) are the designations of stereoisomers of *tris*(bidentate ligand) metal complexes and other octahedral complexes.

Spontaneous resolution is of continued interests since first observed by Louis Pasteur in 1848.^{2c} The interests extend from organic molecules^{4,5,6} to coordination compounds/polymers^{3,7,8,9} metal-organic frameworks (MOFs),^{3,7,10} liquid crystals,¹¹ magneto-chiral compounds,^{8a,e,12} self-assembled monolayers/fibres¹³ and artificial helical structures in supramolecular chemistry.^{3,4,14} The synthesis of chiral metal-complexes from achiral ligands *via* spontaneous resolution touches on the origin of chirality in, for example, biological systems^{15a} and is characteristically linked to the concepts of crystal engineering.^{3d}

Spontaneous resolution usually generates a racemic conglomerate, that is, an equimolar mixture of enantiomer-separated homochiral crystals with the crystals ensemble as a whole being racemic.^{3,12a,14c} In rare cases enantiopure materials can be obtained by homochiral seeding if there is also an equilibrium between the enantiomeric forms in solution.^{7e,8e,15c} Jacques et al. reported that, statistically, only 5 - 10% of all racemates yield to spontaneous resolution forming a racemic conglomerate of homochiral crystals (Scheme 1).^{2a,16a} This may indicate that homochiral interaction is weaker than the heterochiral one between enantiomers.^{17a} It may also indicate that the packing of heterochiral (opposite) enantiomers results in a better space filling and crystal packing index than the packing of homochiral (pure) enantiomers due to center or plane of

symmetry (i.e., inversion or glide symmetry). In other words, the racemic crystals (heterochiral) generally are more stable and slightly denser than the corresponding homochiral crystals – which accounts for the greater incidence of racemic crystals over conglomerates. This is termed Wallach's rule.¹⁸ Brock et al. showed that this tendency is not necessarily thermodynamic in origin, but rather likely reflects both kinetic factors dealing with molecular interactions leading to nucleation and crystal growth from racemic solution, and a greater extent of packing arrangements in achiral crystallographic space groups that might statistically favor racemic crystals over conglomerates.^{17a}

A theoretical examination however indicated that homochiral crystals are the thermodynamically stable phase for 19% of the examined compounds, indicating that the prevalence of stable conglomerates is underestimated.¹⁹ MacDonald et al.^{17b} recently reported that the conglomerates (homochiral) exhibit slightly greater thermal stability than the racemic one (heterochiral) (i.e., $\Delta(\Delta H_{fus.}) = 4.0$ kJ/mol) despite having considerably lower density ($\Delta\rho_{calc.} = 3.7\%$) and less efficient molecular packing in accordance with Wallach's Rule. The greater stability reflects stronger hydrogen-bonding interactions via homochiral packing as compared to heterochiral packing in racemic crystals. Still, the formation of conglomerates vs. racemates is not yet fully understood, therefore the formation of racemic conglomerates (spontaneous resolution) cannot be predicted a priori.^{3a,12a-b,20}

The racemic solution mixture can spontaneously resolve during crystallization to form the racemic conglomerate (enantiomers) due to noncovalent interactions such as strong or weak hydrogen-bonds (e.g., O–H...O/N/S/Cl, C–H...Cl and N–H...O),^{3,4,5d,6b,9,21a} C–H...O and C–H... π interactions,^{5,15b,16b,22} π ... π stacking,^{3,6c,9d,15b,21b} coordination covalent bonds,^{9a-b,11b,14b,23a} and electrostatic and charge transfer bonds (e.g., ion... π /X–H... π , X = O, N, halogen),^{5a,6a-b,23b}. Further, metal-ligand interactions coupled with the interligand steric interactions,^{9c} interchain coordination bond,^{23a} conformational flexibility and bridging nature of ligands,^{7e,12b,21} crystal solvent and temperature (e.g., reaction conditions)^{7e,14e,16b-c} play an important role in the process. Spontaneous resolution requires an efficient transfer of stereochemical information between the neighbours.

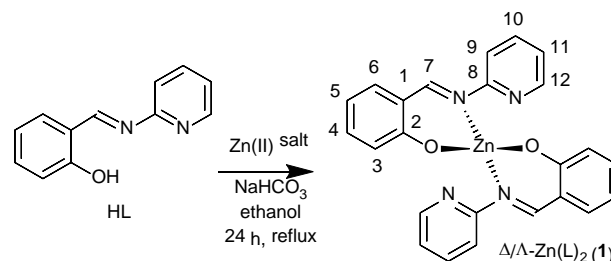
It has recently been reported that when molecules interact, the electronic charges in each of them are redistributed. In chiral molecules, charge redistributions are accompanied by spin polarization, which add an enantioselectivity term to the interaction forces, so that homochiral interaction energies differ significantly from heterochiral ones. As a result, interactions between chiral molecules are less repulsive for molecules of alike chirality (homochiral) than for the molecules of opposite chirality (heterochiral).²⁴

Our previous studies along spontaneous resolution demonstrate that the racemate [Rh(η^4 -cod)(*R,S*-N-phenylglycinate)] spontaneously resolved into the enantiomeric *S*- and *R*-forms, arranged in homochiral *P* (right)- and *M* (left)-helices, crystallizing in the opposite chiral space groups $P4_1$ and $P4_3$, respectively.^{25,26} Intermolecular N–H...O hydrogen bonding interactions connect only the molecules of same *S*- or *R*-configuration into *P* (right)- or *M* (left)-helical chains. Two neighboring homochiral *P* (right)- or *M* (left)-handed helical

chains are interlocked with the corrugated van-der-Waals surface interactions. We report herein the spontaneous resolution of Δ/Λ -bis[N-2-(pyridyl)salicylaldiminato- κ^2 N,O]zinc(II) to a racemic conglomerate as a rare example that such spontaneous resolution can originate *via* weak intermolecular C–H...O hydrogen bonding interactions.

Results and Discussion

The achiral Schiff base ligand N-2-(pyridyl)salicylaldimine (HL) reacts with zinc(II) acetate or nitrate to give Δ/Λ -bis[N-2-(pyridyl)salicylaldiminato- κ^2 N,O]zinc(II), Δ/Λ -Zn(L)₂ (**1**) in the presence of NaHCO₃ under reflux in ethanol (Scheme 2). Vibrational spectra show very strong bands at 1620 and 1609 cm⁻¹ (ν C=N) for the azomethine group.^{27,28,29} EI mass spectrum gives the parent ion peak at 458 ([M]⁺) together with the peak at 199 ([HL+H]⁺). The spectrum further shows several ions peaks for the [M–C₅H₄N]⁺, [M–C₆H₄(OH)(CHN)]⁺, [M–L]⁺ and [C₅H₄N]⁺ species. ¹H NMR spectra (Figure S1 in the ESI[†]) show singlets at δ 9.47 (HL) and 9.44 ppm (**1**) for the imine proton and at δ 13.49 ppm (HL) for the phenolic proton. The aromatic proton adjacent to the pyridine nitrogen atom is found downfield at δ 8.54 (HL) and 8.38 ppm (**1**) due to strong inductive effect of the nitrogen atom. The spectra further show several aromatic protons peaks at δ 6.90–7.80 ppm in HL, which shift to relatively upfield upon coordination to the zinc ion (δ 6.70–7.60 ppm). Cyclic voltammograms demonstrate a weak reduction peak at *ca.* –0.30 V due to the [Zn(L)₂]/[Zn(L)₂][–] couple in acetonitrile (Figure S2 in the ESI[†], see the ESI[†] for details).



Scheme 2 Synthetic route to the formation of Δ/Λ -bis[N-2-(pyridyl)salicylaldiminato- κ^2 N,O]zinc(II) (**1**).

Solid state structural analyses

Two deprotonated N,O-chelate ligands (L[–]) form a pseudo-tetrahedral N₂O₂-coordination sphere around the zinc atom in distorted tetrahedral geometry (Fig. 1). The zinc atom sits on the special position of a 2-fold rotation axis (Fig. S7a in the ESI[†]) so that only one chelate ligand is crystallographically unique. The Zn–O/N bond lengths and angles (Table S2 in the ESI[†]) are as expected from reported literatures for the analogous distorted-tetrahedral Zn(II)-N,O-chelate complexes.^{28,30,48} The optimized structures by DFT show comparable bond lengths and angles to the experimental values (Fig. S8 and Table S2 in the ESI[†]). The O1–Zn1–O1[–] angle is larger by *ca.* 11°, while O1[–]–Zn1–N1 is slightly smaller by *ca.* 4° in the optimized structures. The distortion from tetrahedral geometry and strong deviation from tetrahedral angles at zinc atom is brought upon by the chelate bite angle (O–Zn–N = ~94°) and additional weak coordination of the

two pyridyl-nitrogen atoms to the zinc atom which extends the coordination number to 4+2.⁴⁷ The Zn-N_{pyridyl} bonds are, however, substantially longer (~ 2.82 Å) than the Zn-N_{imine} bonds (~ 2.0 Å) (Table S2 in the ESI†).

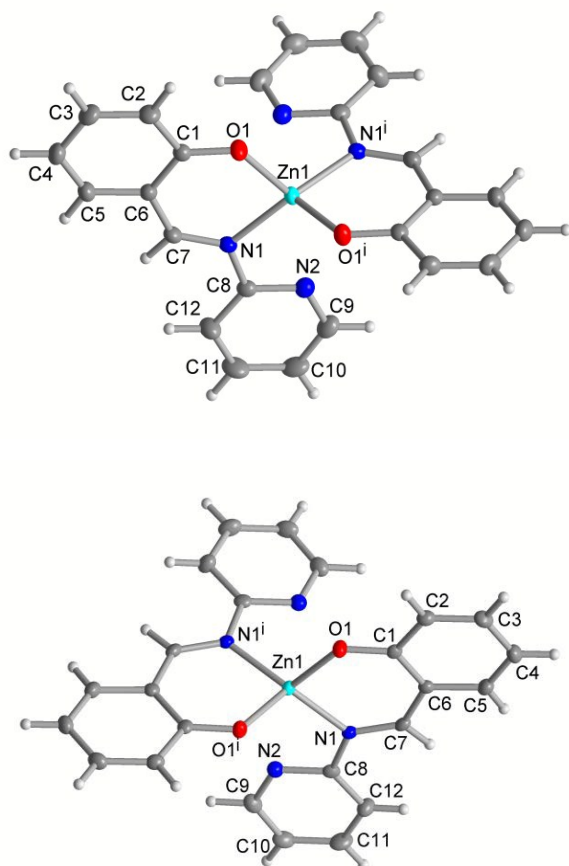
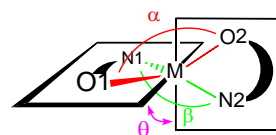


Fig. 1 Molecular structures (50% thermal ellipsoids) of the (top) Λ -form (data set **1g**, 140 K) and (bottom) Δ -configured complexes (data set **1e**, 95 K) with the oxygen atoms are facing to the front. Symmetry transformation (i) $y, x, 1-z$ and $y, x, 2-z$, respectively.

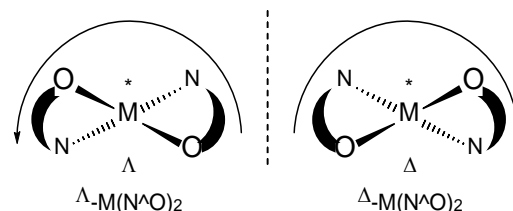
For a more quantitative assessments of the coordination geometry, along with the DFT optimization, the degree of distortion from tetrahedral can be expressed by the dihedral angle θ° (angle between two planes formed by N,O-chelate with the metal atom, that is, N1–Zn–O1 and N1ⁱ–Zn–O1ⁱ), its normalized value $\tau_{\text{tet-sq}}$ ($= \theta/90^\circ$) or the geometry index τ_4 ($\{= (360^\circ - (\alpha + \beta))/141^\circ\}$) (Scheme 3 and Table S3 in the ESI†).^{27–29,31} The value of θ is 90° for tetrahedral and 0° for square-planar geometry (not considering the inherent distortion induced by the chelate ring formation), while $\tau_{\text{tet-sq}}$ and τ_4 values vary from 1.0 (tetrahedral) to zero (square-planar geometry). In compound **1** these values are $\theta \approx 87^\circ$, $\tau_{\text{tet-sq}} \approx 0.97$ and $\tau_4 \approx 0.80$, which are very close to the optimized structures (i.e., 83° , 0.92 and 0.81 , respectively, see Table S3 in the ESI†).

In tetrahedral or pseudo-tetrahedral C_2 -symmetrical metal complexes, two asymmetric N[∧]O-chelate ligands will give rise to metal-centered Λ - and Δ -chirality (i. e., opposite configuration at the metal center), and provide two enantiomers Λ -M(N[∧]O)₂ and Δ -M(N[∧]O)₂ (Scheme 4).^{26–29}



	$\theta/^\circ$	$\tau_{\text{tet-sq}} = \theta/90^\circ$	$\tau_4 = [360^\circ - (\alpha + \beta)]/141^\circ$
tetrahedral	90	1	1
square planar geometry	0	0	0

Scheme 3 Assessments of distortions from tetrahedral to square-planar geometry by θ , $\tau_{\text{tet-sq}}$ and τ_4 , respectively (α and β are the two largest angles in the four-coordinated species, see Table S2 in the ESI†). Dihedral angle θ or its normalized index $\tau_{\text{tet-sq}}$ is preferred for the bis-bidentate chelate complexes. Indeed, the index τ_4 fails to assess correctly a tetrahedral geometry because of existing distortion resulting from chelate ring formation. With chelate ligands, the two largest angles are already larger than 109.5° , thus $\tau_4 < 1.0$, even if the dihedral planes are perfectly perpendicular.^{26–29}



Scheme 4 Induced chirality by N[∧]O-chelate ligands at metal center with Λ (left)- and Δ (right)-handed enantiomers in C_2 -symmetrical tetrahedral or pseudo-tetrahedral geometry.

The chiral zinc complex **1** crystallizes in the tetragonal, chiral space groups $P4_12_12$ and $P4_32_12$, respectively^{32,33} with spontaneous resolution of the (homochiral) single crystals to a racemic conglomerate. The crystal structure refinement data for the absolute structures and determined Flack parameters between $-0.005(2)$ and $0.03(2)$ (Table 1)³⁴ indicate that the individual investigated crystals are enantiopure (homochiral). A Flack parameter close to zero confirms the correct absolute structure and excludes the presence of complexes with opposite metal chirality within the investigated crystal in significant amounts.

The chiral space groups $P4_12_12$ and $P4_32_12$ form an enantiomorphous pair.^{32,33} It was not possible to visibly distinguish the crystals with the Δ - and Λ -configurations or $P4_1$ - and $P4_3$ -helices, respectively (cf. Fig. S11 in the ESI†). So, we performed full crystallographic data set collections on eight crystals to determine the space group. From the investigated overall eight crystals, five of them (**1a–1c**, **1g–1h**) were found to contain the Λ -configured complex in $P4_32_12$ (M -helices) and three of them (**1d–1f**) contained the Δ -configured complex in $P4_12_12$ (P -helices). We thereby also conclude that the crystals present a racemic conglomerate and that no crystalline racemate was present. The 4-fold screw axes run parallel to the c axis, bisecting the a and b axes (Fig. S7b in the ESI†). Fig. 2a illustrates the assembly of the molecular complexes around such a 4-fold helical axis. The molecules from neighbouring helices fit into each other with their corrugated van-der-Waals surfaces (Fig. 2b).^{25,26}

We note that it appears, at first sight, somewhat artificial to speak of "helices formed by the molecules of **1**" as there are no immediately apparent special or stronger supramolecular interactions along the chain axis. The molecular complexes in **1**

have no functional groups for strong hydrogen bonding interactions. A supramolecular packing analysis by PLATON does not indicate any π - π interactions between the aromatic ligands. All centroid-centroid contacts of the aromatic rings are above 4.7 Å, while significant π -stacking should show rather short centroid-centroid contacts (<3.8 Å) with near parallel ring planes.^{35,36} PLATON reveals only one significant C-H... π

contact with less than 2.7 Å for the (C-)H...ring centroid distances and C-H...Cg > 145°,³⁷ albeit to a molecule from an adjacent chain (Fig. S9 and Table S4 in the ESI†). Along the helical-chain arranged molecules only two C-H...O hydrogen bonds are found between consecutive molecules (Figs. 2a, S9 and Tables S5, S6 in the ESI†).³⁸

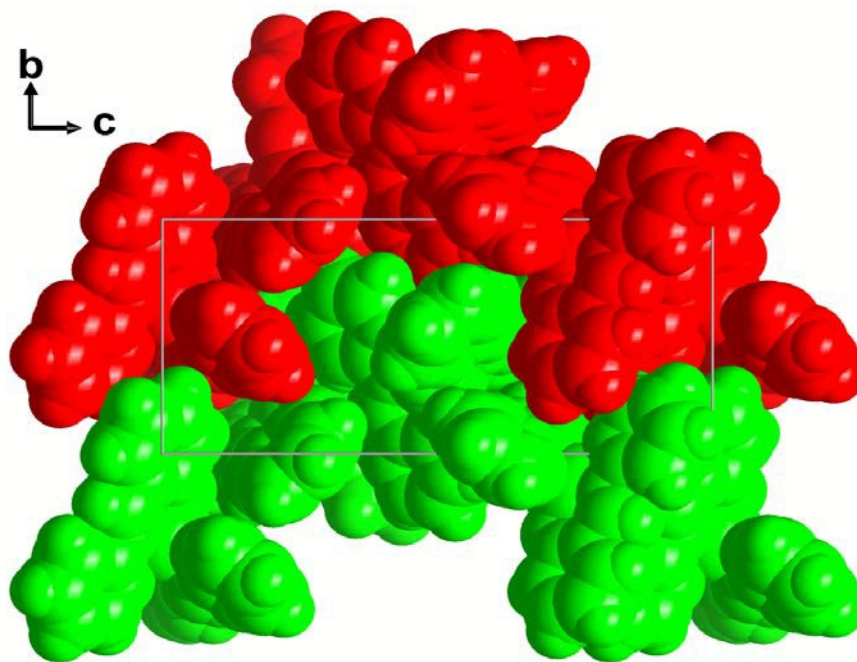
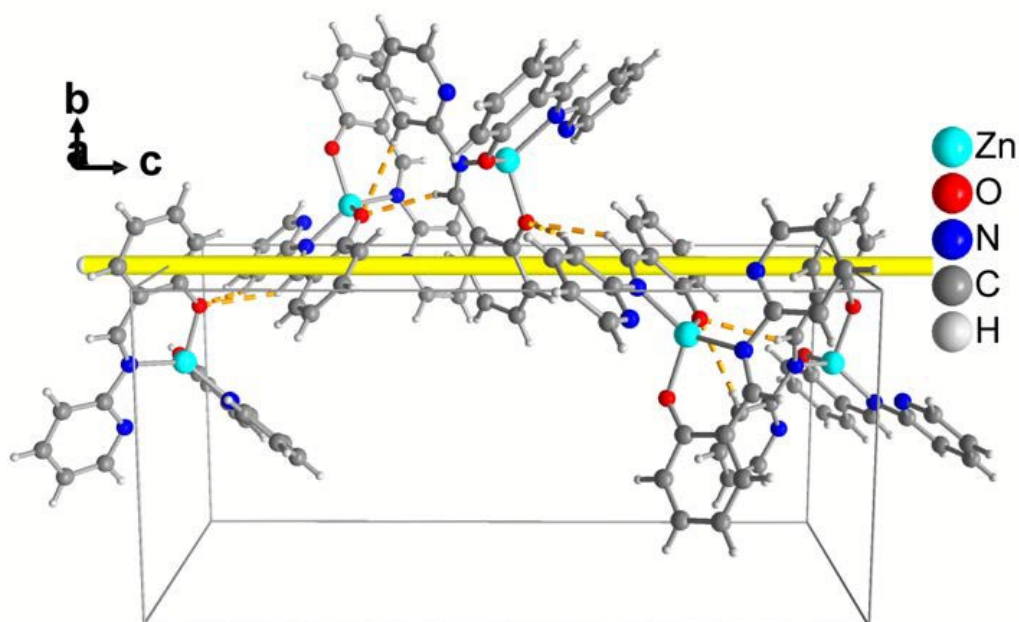


Fig. 2 (a) Assembly of five molecules of **1** (Δ -configuration) winding around the 4_1 (P , right-handed) helix (yellow line). The C-H...O hydrogen bonds are indicated as dashed orange lines (from data set **1e**). (b) The interlocking of two neighboring right (Δ)-handed helical chains in **1** with the corrugated van-der-Waals surface through weak interactions; space-filling representation of the molecules, which are differentiated by red and green in their different helices (from data set **1e**).

Cite this: DOI: XX.XXXX/x0xx00000x

www.rsc.org/xxxxxx

PAPER

The supramolecular packing in **1** is further supported by the analyses of intermolecular interactions with Hirshfeld surfaces using the program CrystalExplorer,³⁹ following the methodology outlined in references.⁴⁰ The 2D fingerprint plot with the characteristic features due to the C–H...O and C–H... π contacts is shown in Fig. 3a. The plot represents an overlay of all contributions from close intermolecular contacts. Fig. 3b illustrates the Hirshfeld surface mapped with the d_{norm} property. The relative contributions to the Hirshfeld surface area due to close intermolecular contacts are C...C (i.e. π ... π) 1.1%, C...H (i.e. C–H... π) 40.7%, C–H...O 11.1% and H...H 38.9% (for details see Fig. S10 in the ESI†).

It is not straightforward to rationalize the homochiral packing in **1** from the rather weakly attracting C–H...O and seemingly insignificant C–H... π interactions. Therefore, we argue that the H...H contacts are considered less repulsive between homochiral than between heterochiral molecules. It has recently been

reported that the interactions between chiral molecules lead to spin polarization *via* charge redistribution that enforce symmetry constraints on the recognition process between two molecules. These constraints can lead to a selectivity in the interaction between enantiomers based on their handedness. As a result, homochiral interaction energies differ from heterochiral ones. Thus interaction is less repulsive for molecules of alike chirality (homochiral) than for molecules of different chirality (enantiomers).²⁴ As an example, the repulsive interaction energy for the methyl groups on homochiral molecules is calculated significantly smaller from that found for the methyl groups on heterochiral molecules at a C...C distances below 3.0 Å (e.g. by about 0.5 kcal/mol at 2.6 Å). Thereby it is important that the interacting groups do not have to be chiral. Chiral recognition occurs because of the spin polarization which is due to the chirality of the molecule as a whole.²⁴

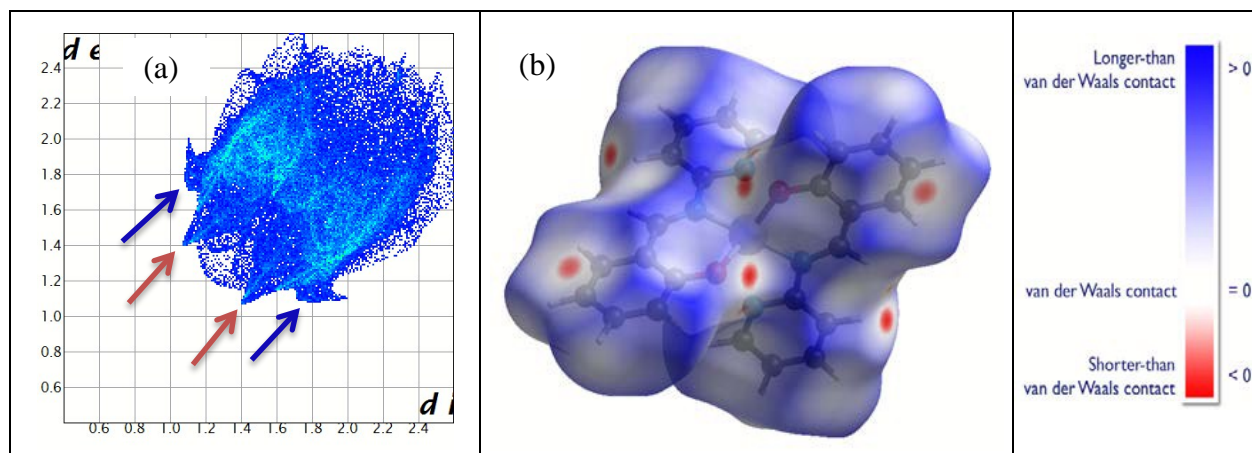


Fig. 3 (a) Graphical presentation of Hirshfeld surface with 2D fingerprint plot with the characteristic features due to the C–H...O (red arrows) and C–H... π (blue arrows) contacts (d_i and d_e are the distances from the surface to the nearest atom interior and exterior to the surface, respectively). (b) Hirshfeld surface mapped with the d_{norm} property the red spots represent the closest contacts and blue the most distant contacts.

A few examples have been reported where the conglomerate formation appears to be controlled by similar weak C–H... π interactions (Ag–N',N'-bis[1-(imidazol-4-yl or pyridin-2-yl)methylidene]benzil-dihydrazone crystallizing in the enantiomorphic space groups $P3_121$ and $P3_221$),^{14f} π – π stacking ([Zn(L)Cl₂]_n or [Hg(L)Br₂]_n, L = 2,5-diphenyl-3,4-di(3-pyridyl)cyclopenta-2,4-dien-1-one, forms colonies of homochiral *M*-helix – space group $C2$),^{6c} C–H... π and C–H...N interactions (Cu-bi(pyridyl)triazolate crystallizing in 4₁-helical structure – space group $P4_32_12$),⁴¹ C–H...Cl interactions (homochiral 1D-helical metal–organic framework in α,α' -bis(pyrazolyl)-*m*-xylylene zinc(II) chloride – space group $P2_1$),²¹ and C–H...O and/or C–H... π interactions (kinetically controlled helical supramolecular structure of *myo*-Inositol hexabenzate – space group $P6_1$)⁴² and thermodynamically controlled helical structure of 2,3:6,7-dibenzobicyclo[3.3.1]nona-2,6-diene-4,8-dione – space

group $P2_12_12_1$)^{16b}). We note that many of such homochiral crystal packings with weak controlling interactions (as in **1**) seem to feature simultaneous helical arrangements.^{5,9c,15b,21,43} For preferential and extended homochiral interactions between the neighbouring helices *via* noncovalent interactions, the chirality will extend to a higher dimensionality, which enhances the probability of spontaneous resolution.^{5d,8e,10a,12,44,45}

Thermal analysis

The thermodynamic parameters of racemic crystals (heterochiral) will differ from racemic conglomerates (homochiral).^{17b} To further support the notion that the crystal batch presents solely a racemic conglomerate and that no crystalline racemate was present we carried out a dynamic scanning calorimetry (DSC) measurement. If both types of crystals would be present DSC may show a binary phase by two different phase transitions for

the melting or decomposition of homochiral and heterochiral crystals.^{28,46,47} The DSC heating curve (Fig. S3 in the ESI†) exhibits a single-phase transformation at *ca.* 260 °C ($\Delta H = -36.5$ kJ/mol) which we see as evidence for having only one type, name
5 the homochiral crystals in the racemic conglomerate in accordance with the X-ray analyses (where only homochiral crystals are found, *vide supra*).

Electronic and computed spectra.

The electronic spectra of the free ligand (HL) and complex (**1**) in chloroform (Fig. S4 and Table S1 in Supp. Info.) feature several identical bands/shoulders below 390 nm for intra-ligand $n \rightarrow \pi^*$ and $\pi \rightarrow \pi^*$ transitions (LL), respectively. An additional broad band above 390 nm with absorption maxima at 416 nm is found in **1**, due to metal-ligand (ML) charge transfer transitions.^{28,47,48}
15 Time dependent electronic spectra (Fig. S5 in the ESI†) show decomposition of the compound upon dissolution in chloroform (*ca.* 10% within 5 min. or 100% within 2 hours), a common feature of the labile distorted-tetrahedral Zn(II)-N,O-chelate complexes.^{28,47-48}

To gain further insight on the Δ/Λ -chirality at-metal (i.e., spontaneous resolution) we attempted to measure electronic circular dichroism (ECD) spectra. Because the crystals of **1** are a racemic conglomerate the overall crystal mixture behaves like a racemate. Thus, measuring an ECD spectrum of the crystal
25 mixture in the solid-state or in solution would show no enantiomer signal. Only if we measure the ECD spectrum of a single (tiny) crystal in the solid state or as a very dilute solution we would possibly be able to see the ECD pattern of the single enantiomer. It was not feasible to run ECD for a single crystal in the solid state with the instrument available to us. In solution, we conducted ECD-measurements for a single crystal (four attempts, each with a single crystal) or several crystals (two attempts, each with 3-4 crystals for higher concentration) in CHCl_3 . In all attempts the ECD spectra look rather similar and the solutions
30 appear ECD-inactive (Figure S12 in the ESI†). This may indicate either a too low concentration of the enantiomeric species or racemization due the absence or loss of the weak supramolecular interactions which had led to spontaneous resolution in the solid state. In earlier work we have already shown the helicity inversion of similar four-coordinated nonplanar Zn(II) and Cu(II) Schiff-base complexes in solution,^{49,50} which can occur through the planar conformation.

The computed electronic spectra by TD-DFT (Fig. S4 in the ESI†) for both $P4_1(\Delta)$ - and $P4_3(\Lambda)$ -enantiomers of the compound are identical and show the best fit to the experimental one (see the ESI† for details on computed spectra).
45

Conclusions

The enantiomorphous complex Λ/Δ -bis[N-2-(pyridyl)salicylaldiminato- $\kappa^2\text{N,O}$]zinc(II) (**1**) crystallizes to a racemic conglomerate
50 *via* spontaneous resolution during crystallization. The Δ -configured molecular complexes in **1** assemble in right (*P*)- and the Λ -configured ones into left (*M*)-handed 4₁- and 4₃-helical chain, respectively. Only molecules of the same (Δ or Λ)-configuration are combined into a chain and subsequently only
55 chains of the same 4₁- or 4₃-handedness are found in a homochiral crystal. This resolution occurs in the absence of

strong (classical) hydrogen bonding or π - π stacking. Instead, the resolution and helical chain orientation seems be controlled solely through C-H...O hydrogen bonding to neighbouring molecules
60 along the chain axis. C-H...O hydrogen bonding is normally considered one of the weakest supramolecular (noncovalent) interactions. The results reflect apparently a higher stability for the racemic conglomerate (homochiral crystals) in the absence of any strong interactions. This may also correspond to a more
65 efficient packing in the homochiral crystals, opposite to Wallach's rule.

Further, we invoke a less repulsive interactions between homochiral than between heterochiral molecules because of spin polarization and see it as remarkable that such weak
70 supramolecular interactions can drive spontaneous resolution.

Experimental section

All the reagents and solvents were obtained from commercial sources and used without further purification. FT-IR-spectra were recorded on a Nicolet iS10 spectrometer as KBr discs at ambient
75 temperature. Electronic spectra were obtained with a Shimadzu UV 1800 spectrophotometer in cyclohexane at 25 °C. Elemental analyses were done on a Vario EL instrument from Elementaranalysensysteme GmbH. Thermal analysis was performed on a SHIMADZU DSC-60 differential scanning
80 calorimeter (DSC) under nitrogen gas at 40–260 °C (just before the decomposition temperature) and heating rate of 10 K min⁻¹. An Epsilon™ Instruments (BASi) electrochemical analyzer was used for cyclic voltammetry (CV) experiments in acetonitrile containing tetra-*N*-butyl-ammonium-hexafluorophosphate (TBAP)
85 as supporting electrolyte. The three-electrode measurement was carried out at 298 K with a platinum disc working electrode, a platinum wire auxiliary electrode and an Ag/AgCl reference electrode. The solution containing the complex and TBAP was deoxygenated for 10 minutes with nitrogen gas. ¹H NMR spectra
90 were recorded on a Bruker Avance DPX 300 spectrometer at 300 MHz in CDCl_3 at 20 °C. ECD spectra of single crystals or a few crystals were run with an Olis RSM100 Spectropolarimeter in chloroform (0.1 mL, sufficient color) at 20 °C. The EI mass spectrum was obtained on a Finnigan Trace GC Ultra. Isotopic
95 distributions patterns for ^{64/66/68}Zn(II)-containing ions are clearly visible in the mass spectrum.

Synthesis of the Schiff base ligand (HL)

Salicylaldehyde (1.730 g, 14.18 mmol) was dissolved in 10 mL of methanol, 2-3 drops of concentrated H_2SO_4 were added and the
100 solution stirred for 10 min. An equimolar amount of 2-aminopyridyl (1.332 g, 14.17 mmol) was added into this solution. The reaction mixture was then refluxed for 6 h, and the colour turned to bright yellow. The solvent was evaporated to 50% in *vacuo*, and the solution was left standing for crystallisation at room
105 temperature. The crystals were filtered off and washed three times with methanol (5 mL in each). The bright yellow crystals of N-2-(pyridyl)salicylaldimine (HL) were dried in air for 2 d.

N-2-(pyridyl)salicylaldimine (HL). Yield: 2.35 g (84%). IR (KBr, cm^{-1}): $\nu = 3051, 2975\text{w}$ (C-H), 1608, 1588vs (C=N), and
110 1574s (C=C). MS (EI, 70 eV): m/z (%) = 199 (100) $[\text{M}+\text{H}]^+$. ¹H NMR (CDCl_3 , 300 MHz): $\delta = 6.98$ (dt, $J_{\text{HH}} = 7.5$ Hz, $J_{\text{HH}} = 0.9$ Hz, 1H, H_5), 7.06 (d, $J_{\text{HH}} = 8.1$ Hz, 1H, H_3), 7.25 (ddd, $J_{\text{HH}} = 6.0$

Hz, $J_{HH} = 0.9$ Hz, 1H, H_4), 7.36 (d, $J_{HH} = 7.8$ Hz, 1H, H_6), 7.43 (ddd, $J_{HH} = 7.2$, 6.9 Hz, $J_{HH} = 1.8$, 1.2 Hz, 1H, H_{11}), 7.53 (dd, $J_{HH} = 7.5$, 7.8 Hz, $J_{HH} = 1.5$, 1.8 Hz, 1H, H_9), 7.80 (dt, $J_{HH} = 7.8$, 7.5 Hz, $J_{HH} = 2.1$, 1.8 Hz, 1H, H_{10}), 8.54 (dd, $J_{HH} = 4.5$, 4.8 Hz, $J_{HH} = 1.2$, 1.5 Hz, 1H, H_{12}), 9.47 (s, 1H, H_7), and 13.49 (s, 1H, OH) (see Scheme 1 for atom numbering).

Synthesis of compound 1

Two equivalents of *N*-2-(pyridyl)salicylaldimine (HL) (396 mg, 2.00 mmol) were dissolved in 10 mL of ethanol and added to a solution of zinc(II) acetate or zinc(II) nitrate (1.0 mmol) in 10 mL of methanol or ethanol. Into this solution two equivalents of NaHCO₃ (dissolved in 5 mL of methanol) was added and the mixture refluxed for 24 h. After the solvent volume was reduced to ca. 50% in *vacuo*, the solution was left standing for crystallization by slow solvent evaporation at room temperature. Bright yellow to light orange coloured crystals (see Fig. S11 in the ESI† for crystals data sets **1a–1e**), suitable for X-ray measurement, were obtained within 4–5 days. The crystals were filtered off, washed two times with ethanol (2 ml), and dried in *vacuo* at 30 °C. Alternatively, identical light orange crystals (crystal data set **1g**) were obtained *via* slow diffusion of methanol into a concentrated solution of the dried compound in dichloromethane.

Bis[*N*-2-(pyridyl)salicylaldiminato-κ²N,O]zinc(II), Δ/Λ-Zn(L)₂ (**1**). Yield: 0.25 g (74%). IR (KBr, cm⁻¹): ν = 3080, 3050, 3014m (H-C), 1620, 1609vs, (C=N), and 1585vs (C=C). ¹H NMR (CDCl₃, 300 MHz): δ = 6.73 (t, $J_{HH} = 7.0$ Hz, 1H, H_5), 6.96 (d, $J_{HH} = 8.6$ Hz, 1H, H_3), 7.12 (dd, $J_{HH} = 7.1$, 6.8, $J_{HH} = 1.8$ Hz, 1H, H_4), 7.27 (d, $J_{HH} = 7.4$ Hz, 1H, H_6), 7.42 (d, $J_{HH} = 8.0$ Hz, 2H, $H_{9,11}$), 7.62 (t, $J_{HH} = 7.2$ Hz, 1H, H_{10}), 8.38 (d, $J_{HH} = 3.6$ Hz, 1H, H_{12}), and 9.44 (s, 1H, H_7) (see Scheme 1 for atom numbering). MS (EI, 70 eV): *m/z* (%) = 458 (80) [M]⁺, 380 (10) [M-C₅H₄N]⁺, 338 (40) [M-C₆H₄(OH)(CHN)]⁺, 261 (100) [M-L1]⁺, 198 (20) [HL1]⁺, 197 (25) [HL1-H]⁺, and 78 (55) [C₅H₄N]⁺. C₂₄H₁₈N₄O₂Zn (459.81): calcd C 62.69, H 3.95, N 12.18; found C 63.11, H 3.71, N 12.02.

X-ray Crystallography

Suitable single crystals (crystal data sets **1a–1h**) were carefully selected under a polarizing microscope. *Data collection*: Bruker APEX2 CCD diffractometer (with microfocus tube); sources: Mo-Kα radiation (0.71073 Å) for **1a**, **1e**, **1f**, **1g**, **1h** and Cu-Kα radiation (1.54178 Å) for **1b**, **1c**, **1d**; multilayer mirror, ω- and φ-scan; data collection with Apex2,⁵¹ cell refinement and data reduction with SAINT (Bruker),⁵² experimental absorption correction with SADABS.⁵³ *Structure Analysis and Refinement*: The structures were solved by direct methods using SHELXS-97;⁵⁴ refinement was done by full-matrix least squares on *F*² using the SHELXL-97 program suite.⁵⁴ All non-hydrogen positions were refined with anisotropic displacement parameters. Hydrogen atom positions were found and refined in data sets **1a–1f**, **1h** and positioned geometrically using a riding model in data set **1g**. Crystal data and details on the structure refinement are given in Table 1. Graphics were drawn with the DIAMOND.⁵⁵ Computation on the supramolecular C–H⋯O interactions were carried out using the PLATON for Windows⁵⁶ and Mercury 3.0.⁵⁷ The structural data for this paper have been deposited with the Cambridge Crystallographic Data Center

(CCDC numbers 1844266–1844273).

Computational section

All calculations were performed with the Gaussian 09 software package⁵⁸ The initial geometries for computation were generated from the cif-files having opposite chiral space groups with *P*4₃(Λ) (from data set **1a**)- and *P*4₁(Δ) (from data set **1d**)-enantiomers, respectively. The optimizations were performed by DFT with the B3LYP/6-31g(d) for both enantiomers, respectively. Both optimized structures (Fig. S8 in the ESI†) show the same free energy minima as expected for the equi-stable enantiomers (e.g., -3073.783631 au for *P*4₁-isomer and -3073.783627 au for *P*4₃-isomer). For excited state properties, Time Dependent Density Functional Theory (TD-DFT) was employed with the B3LYP/TZVP on both optimized structures, incorporating PCM (Polarization Continuum Model) using chloroform as a solvent, respectively. For calculations, 72 excited states were considered (Table S7 in the ESI†).

Acknowledgements

We acknowledge the Wazed Miah Science Research Centre (WMSRC) at Jahangirnagar University, Dhaka, Bangladesh for obtaining elemental, ¹H NMR and CV data. Our sincere thanks to Professor Andrew Woolley and Mr. Ryan Woloschuk, Department of Chemistry, University of Toronto, Canada, for running the ECD spectra. ME thanks the Alexander-von-Humboldt (AvH) Foundation, Bonn for its continuous support.

Cite this: DOI: XX.XXXX/x0xx00000x

www.rsc.org/xxxxxx

Table 1. Crystal data for compound **1** (crystal data sets **1a–1h**).

Crystal No.	1a	1b	1c	1d
CCDC no.	1844266	1844268	1844270	1844267
Empirical formula	C ₂₄ H ₁₈ Zn ₁ N ₄ O ₂	C ₂₄ H ₁₈ Zn ₁ N ₄ O ₂	C ₂₄ H ₁₈ Zn ₁ N ₄ O ₂	C ₂₄ H ₁₈ Zn ₁ N ₄ O ₂
<i>M</i> / g mol ⁻¹	459.81	459.81	459.81	459.81
Crystal size / mm ³	0.30 × 0.30 × 0.20	0.37 × 0.28 × 0.24	0.27 × 0.25 × 0.16	0.23 × 0.21 × 0.19
Temperature / K	296(2)	296(2)	296(2)	296(2)
θ range / ° (complet.)	2.26–25.08 (100%)	4.92–65.89 (99.6)	4.92–64.80 (96.8)	4.92–66.00 (98.8)
<i>h</i> ; <i>k</i> ; <i>l</i> range	±11; ±11; -25, 24	±11; ±11; -24, 23	-11, 10; -11, 10; -24, 19	±11; ±11; -24, 25
Crystal system	Tetragonal	Tetragonal	Tetragonal	Tetragonal
Space group	<i>P</i> 4 ₃ 2 ₁ 2			
<i>a</i> = <i>b</i> / Å	9.9154(8)	9.9041(3)	9.9138(3)	9.9077(12)
<i>c</i> / Å	21.343(2)	21.3545(7)	21.3276(8)	21.330(3)
<i>V</i> / Å ³	2098.3(4)	2094.69(11)	2096.15(12)	2093.90(4)
<i>Z</i>	4	4	4	4
<i>D</i> _{calc} / g cm ⁻³	1.455	1.458	1.457	1.459
μ / mm ⁻¹	1.199	1.864	1.862	1.864
<i>F</i> (000)	944	944	944	944
Max./min. transmission	0.795 / 0.715	0.605 / 0.523	0.605 / 0.523	0.753 / 0.620
Reflect. collected	12332	21092	15506	16993
Indep. reflect. (<i>R</i> _{int})	1870 (0.030)	1816 (0.034)	1712 (0.027)	1799 (0.034)
Data/restraints/parameters	1870 / 0 / 177	1816 / 0 / 177	1712 / 0 / 177	1799 / 0 / 177
Max./min. $\Delta\rho$ / e.Å ⁻³ ^a	0.117 / -0.162	0.130 / -0.219	0.135 / -0.235	0.108 / -0.183
<i>R</i> 1/ <i>wR</i> 2 [<i>I</i> > 2 σ (<i>I</i>)] ^b	0.0191 / 0.0485	0.0197 / 0.0507	0.0203 / 0.0538	0.0193 / 0.0502
<i>R</i> 1/ <i>wR</i> 2 (all data) ^b	0.0217 / 0.0505	0.0197 / 0.0507	0.0204 / 0.0539	0.0197 / 0.0509
Good.-of-fit on <i>F</i> ² ^c	1.092	1.134	1.143	1.127
Flack parameter ^d	-0.01(1)	0.02(2)	0.03(2)	0.03(2)

Crystal No.	1e	1f	1g	1h
CCDC no.	1844269	1844271	1844273	1844272
Empirical formula	C ₂₄ H ₁₈ Zn ₁ N ₄ O ₂	C ₂₄ H ₁₈ Zn ₁ N ₄ O ₂	C ₂₄ H ₁₈ Zn ₁ N ₄ O ₂	C ₂₄ H ₁₈ Zn ₁ N ₄ O ₂
<i>M</i> / g mol ⁻¹	459.81	459.81	459.81	459.79
Crystal size / mm ³	0.23 × 0.22 × 0.16	0.26 × 0.14 × 0.13	0.25 × 0.25 × 0.25	0.08 × 0.10 × 0.15
Temperature / K	95(2)	95(2)	140(2)	150(2)
θ range / ° (complet.)	2.29–25.13 (99.5)	2.29–27.58 (99.6)	2.280–27.673 (99.5)	2.278–27.998 (99.9)
<i>h</i> ; <i>k</i> ; <i>l</i> range	±11; ±11; -25, 23	-9, 12; -12, 11; -16, 27	±12; ±12; ±27	±13; ±13; ±27
Crystal system	Tetragonal	Tetragonal	Tetragonal	Tetragonal
Space group	<i>P</i> 4 ₃ 2 ₁ 2			
<i>a</i> = <i>b</i> / Å	9.8258(19)	9.8329(12)	9.8592(4)	9.8663(6)
<i>c</i> / Å	21.005(5)	21.061(2)	21.1220(10)	21.1146(17)
<i>V</i> / Å ³	2027.90(7)	2036.3(4)	2053.14(19)	2055.4(3)
<i>Z</i>	4	4	4	4
<i>D</i> _{calc} / g cm ⁻³	1.506	1.500	1.487	1.486
μ (Mo <i>K</i> α) / mm ⁻¹	1.241	1.236	1.226	1.224
<i>F</i> (000)	944	944	944	944
Max./min. transmission	0.745 / 0.524	0.860 / 0.740	0.746 / 0.669	0.747 / 0.697
Reflect. collected	11665	7224	98896	37194
Indep. reflect. (<i>R</i> _{int})	1807 (0.034)	2344 (0.026)	2388 (0.024)	2477 (0.029)
Data/restraints/parameters	1807 / 0 / 177	2344 / 0 / 177	2388 / 0 / 141	2477 / 0 / 141
Max./min. $\Delta\rho$ / e.Å ⁻³ ^a	0.163 / -0.162	0.277 / -0.321	0.234 / -0.148	0.231 / -0.146
<i>R</i> 1/ <i>wR</i> 2 [<i>I</i> > 2 σ (<i>I</i>)] ^b	0.0156 / 0.0405	0.0235 / 0.0565	0.0161 / 0.0456	0.0178 / 0.0473
<i>R</i> 1/ <i>wR</i> 2 (all data) ^b	0.0164 / 0.0408	0.0266 / 0.0575	0.0163 / 0.0457	0.0187 / 0.0477
Good.-of-fit on <i>F</i> ² ^c	1.080	1.040	1.113	1.137
Flack parameter ^d	0.01(1)	0.00(1)	-0.005(2)	-0.012(3)

^a Largest difference peak and hole. – ^b $R_1 = [\sum(|F_o| - |F_c|)] / \sum |F_o|$; $wR_2 = [\sum [w(F_o^2 - F_c^2)^2] / \sum [w(F_o^2)^2]]^{1/2}$. – ^c Goodness-of-fit = $[\sum [w(F_o^2 - F_c^2)^2] / (n - p)]^{1/2}$. – ^d Absolute structure parameter.³⁴

Notes and references

- ^a Department of Chemistry, Jahangirnagar University, Dhaka-1342, Bangladesh. Email: enamullah@juniv.edu
- ^b Institut für Anorganische Chemie und Strukturchemie, Heinrich-Heine-Universität Düsseldorf, Universitätsstr. 1, D-40225 Düsseldorf, Germany. Email: janiak@uni-duesseldorf.de
- † Electronic Supplementary Information (ESI) available: Figures and analyses of UV-Vis., ¹H NMR, DSC and CV. Tables of excitation properties and selected bond lengths and angles, packing analyses, Hirshfeld surface plots. For ESI† and crystallographic data in CIF or other electronic format see DOI: --
- (a) E. L. Eliel and S. H. Wilen, *Stereochemistry of Organic Compounds*, J. Wiley & Sons, New York, 1994 and references cited therein; (b) J. M. Lehn, *Supramolecular Chemistry: Concepts and Perspectives*, VCH, Weinheim, 1995.
 - (a) J. Jacques, A. Collet and S. H. Wilen, *Enantiomers, Racemates and Resolutions*, Krieger Publishing Company, Malabar, Florida, 1994; (b) E. C. Constable, *Comprehensive Supramolecular Chemistry*, Pergamon, Oxford, 1996; (c) L. Pasteur, *Ann. Chim. Phys.*, 1848, **24**, 442–459.
 - (a) L. Pérez-García and D. B. Amabilino, *Chem. Soc. Rev.*, 2002, **31**, 342–356; (b) L. Pérez-García and D. B. Amabilino, *Chem. Soc. Rev.*, 2007, **36**, 941–967; (c) J. Crassous, *Chem. Soc. Rev.*, 2009, **38**, 830–845; (d) C. Janiak, *Dalton Trans.*, 2003, 2781–2804, and references therein.
 - (a) A. N. Kravchenko, G. K. Kadorkina, A. S. Sigachev, E. Y. Maksareva, K. A. Lyssenko, P. A. Belyakov, O. V. Lebedev, O. N. Kharybin, N. N. Makhova and R. G. Kostyanovsky, *Mendelev Commun.*, 2003, 114–116; (b) E. Alcalde, L. Perez-Garcia, S. Ramos, J. F. Stoddart, A. J. P. White and D. J. Williams, *Mendelev Commun.*, 2004, 233–235; (c) R. G. Kostyanovsky, F. A. Lakhvich, P. M. Philipchenko, D. A. Lenev, V. Y. Torbeev and K. A. Lyssenko, *Mendelev Commun.* 2002, **12**, 147–148.
 - (a) S. Jayanty and T. P. Radhakrishnan, *Chem. Eur. J.*, 2004, **10**, 2661–2667; (b) I. Azumaya, D. Uchida, T. Kato, A. Yokoyama, A. Tanatani, H. Takayanagi and T. Yokozawa, *Angew. Chem., Int. Ed.*, 2004, **43**, 1360–1363; (c) J. N. Moorthy, R. Natarajan and P. Venugopalan, *J. Org. Chem.*, 2005, **70**, 8568–8571; (d) T. B. Norsten, R. McDonald and N. R. Branda, *Chem. Commun.*, 1999, 719–720, and references cited therein.
 - (a) M. Sakamoto, N. Utsumi, M. Ando, M. Saeki, T. Mino, T. Fujita, A. Katoh, T. Nishio and C. Kashima, *Angew. Chem., Int. Ed.*, 2003, **42**, 4360–4363; (b) R. Custelcean and M. G. Gorbunova, *CrystEngComm*, 2005, **7**, 297–301; (c) U. Siemeling, I. Scheppelmann, B. Neumann, A. Stammier, H. -G. Stammier and J. Frelek, *Chem. Commun.*, 2003, 2236–2237.
 - (a) S.-H. Wang, F.-K. Zheng, M.-J. Zhang, Z.-F. Liu, J. Chen, Y. Xiao, A.-Q. Wu, G.-C. Guo and J.-S. Huang, *Inorg. Chem.*, 2013, **52**, 10096–10104; (b) Z. J. Lin, A. Z. Slawin and R. E. Morris, *J. Am. Chem. Soc.*, 2007, **129**, 4880–4881; (c) J. Zhang, S. Chen, T. Wu, P. Feng and X. H. Bu, *J. Am. Chem. Soc.*, 2008, **130**, 12882–12883; (d) G. Durá, M. C. Carrió, F. A. Jaló, A. M. Rodríguez and B. R. Manzano, *Cryst. Growth Des.*, 2013, **13**, 3275–3282; (e) S. Zang, Y. Su, Y. Li, Z. Ni and Q. Meng, *Inorg. Chem.*, 2006, **45**, 174–180.
 - (a) X.-L. Tong, T.-L. Hu, J.-P. Zhao, Y.-K. Wang, H. Zhang and X.-H. Bu, *Chem. Commun.*, 2010, **46**, 8543–8545; (b) K. K. Bisht, E. Suresh, *J. Am. Chem. Soc.*, 2013, **135**, 15690–15693; (c) M. Sasa, K. Tanaka, X.-H. Bu, M. Shiro and M. Shionoya, *J. Am. Chem. Soc.*, 2001, **123**, 10750–10751; (d) G.-C. Ou, L. Jiang, X.-L. Feng and T.-B. Lu, *Inorg. Chem.*, 2008, **47**, 2710–2718; (e) G. Tian, G.-S. Zhu, X.-Y. Yang, Q.-R. Fang, M. Xue, J.-Y. Sun, Y. Wei and S.-L. Qiu, *Chem. Commun.*, 2005, 1396–1398.
 - (a) R. Kramer, J.-M. Lehn, A. De Cian and J. Fischer, *Angew. Chem., Int. Ed.*, 1993, **32**, 703–706; (b) F. M. Tabellion, S. R. Seidel, A. M. Arif and P. J. Stang, *Angew. Chem., Int. Ed.*, 2001, **40**, 1529–1532; (c) X. Chen, M. Du and T. C. W. Mak, *Chem. Commun.*, 2005, 4417–4419; (d) J. Breu, H. Domel and A. Stoll, *Eur. J. Inorg. Chem.*, 2000, 2401–2408.
 - (a) B. Gil-Hernández, H. Höpfe, J. K. Vieth, J. Sanchiz and C. Janiak, *Chem. Commun.*, 2010, **46**, 8270–8272; (b) R. E. Morris and X. Bu, *Nat. Chem.*, 2010, **2**, 353–361; (c) K. K. Bisht and E. Suresh, *Inorg. Chem.*, 2012, **51**, 9577–9579; (d) Q.-Y. Liu, Y.-L. Wang, N. Zhang, Y.-L. Jiang, J.-J. Wei and F. Luo, *Cryst. Growth Des.*, 2011, **11**, 3717–3720; (e) X.-D. Zheng, M. Zhang, L. Jiang and T.-B. Lu, *Dalton Trans.*, 2012, **41**, 1786–1791.
 - (a) D. M. Walba, E. Körblöva, R. Shao, J. E. Maclellan, D. R. Link, M. A. Glaser and N. A. Clark, *J. Phys. Org. Chem.*, 2000, **13**, 830–836 and references cited therein; (b) Y. Takanishi, H. Takezoe, Y. Suzuki, I. Kobayashi, T. Yajima, M. Terada and K. Mikami, *Angew. Chem., Int. Ed.*, 1999, **38**, 2354–2356; (c) K. Mikami, T. Yajima, J. Kojima, M. Terada, S. Kawauchi, H. Shirasaki, K. Okuyama, Y. Suzuki, I. Kobayashi, Y. Takanishi and H. Takezoe, *Mol. Cryst. Liq. Cryst.*, 2000, **346**, 41–49.
 - (a) E.-Q. Gao, S.-Q. Bai, Z.-M. Wang and C.-H. Yan, *J. Am. Chem. Soc.*, 2003, **125**, 4984–4985; (b) E.-Q. Gao, Y.-F. Yue, S.-Q. Bai, Z. He and C.-H. Yan, *J. Am. Chem. Soc.*, 2004, **126**, 1419–1429; (c) F. Pointillart, C. Train, K. Boubekeur, M. Gruselle and M. Verdager, *Tetrahedron: Asymmetry*, 2006, **17**, 1937–1943.
 - (a) I. Weissbuch, I. Kuzmenko, M. Berfeld, L. Leiserowitz and M. Lahav, *J. Phys. Org. Chem.*, 2000, **13**, 426–434, and references cited therein; (b) H. Fang, L. C. Giancarlo and G. W. Flynn, *J. Phys. Chem. B.*, 1998, **102**, 7311–7315; (c) P. Qian, H. Nanjo, T. Yokoyama, T. M. Suzuki, K. Akasaka and H. Orhui, *Chem. Commun.*, 2000, 2021–2022; (d) J. Sly, P. Kasak, E. Gomar-Nadal, C. Rovira, L. Gorriz, P. Thordarson, D. B. Amabilino, A. E. Rowan and R. J. M. Nolte, *Chem. Commun.*, 2005, 1255–1257; (e) M. Takeuchi, S. Tanaka and S. Shinkai, *Chem. Commun.*, 2005, 5539–5541.
 - (a) A. Erxleben, *Inorg. Chem.*, 2001, **40**, 412–414; (b) T. Ezuhara, K. Endo and Y. Aoyama, *J. Am. Chem. Soc.*, 1999, **121**, 3279–3283; (c) I. Katsuki, Y. Motoda, Y. Sunatsuki, N. Matsumoto, T. Nakashima and M. Kojima, *J. Am. Chem. Soc.*, 2002, **124**, 629–640; (d) K. Biradha, C. Seward and M. J. Zaworotko, *Angew. Chem., Int. Ed.*, 1999, **38**, 492–495; (e) C.-Y. Chen, P.-Y. Cheng, H.-H. Wu and H.-M. Lee, *Inorg. Chem.*, 2007, **46**, 5691–5699.
 - (a) L. M. Foroughi and A. J. Matzger, *Nat. Chem.*, 2011, **3**, 663–665; (b) Q. Sun, T. Bai, G. He, C. Duan, Z. Lin, Q. Meng, *Chem. Commun.*, 2006, 2777–2779; (c) A. Johansson and M. Hakansson, *Chem. Eur. J.*, 2005, **11**, 5238–5248.
 - (a) J. Jacques, M. Leclercq and M.-J. Brienne, *Tetrahedron*, 1981, **37**, 1727–1733; (b) P. A. Levkin, Y. A. Strelenko, K. A. Lyssenko, V. Schurig and R. G. Kostyanovsky, *Tetrahedron: Asymmetry*, 2003, **14**, 2059–2066; (c) P. A. Levkin, E. Schweda, H. J. Kolb, V. Schurig and R. G. Kostyanovsky, *Tetrahedron: Asymmetry*, 2004, **15**, 1445–1450.
 - (a) C. P. Brock, W. B. Schweizer and J. D. Dunitz, *J. Am. Chem. Soc.*, 1991, **113**, 9811–9820; (b) P. S. Navare and C. MacDonald, *Cryst. Growth Des.*, 2011, **11**, 2422–2428; (c) A. R. Kennedy, C. A. Morrison, N. E. B. Briggs and W. Arbuckle, *Crystal Growth Des.*, 2011, **11**, 1821–1834.
 - (a) O. Wallach, *Liebigs Ann. Chem.*, 1895, **286**, 90–143; (b) K.-H. Ernst, *Israel J. Chem.*, 2017, **57**(1–2) 24–30.
 - A. Otero-de-la-Roza, J. E. Hein and E. R. Johnson, *Crystal Growth Des.*, 2016, **16**, 6055–6059.
 - (a) R. Kuroda and S. F. Mason, *J. Chem. Soc., Dalton Trans.*, 1981, 1268–1273; (b) C. P. Brock, J. D. Dunitz, *Chem. Mater.*, 1994, **6**, 1118–1127.
 - (a) V. Balamurugan and R. Mukherjee, *CrystEngComm*, 2005, **7**, 337–341; (b) M.-C. Blum, E. Cavar, M. Pivetta, F. Patthey and W.-D. Schneider, *Angew. Chem., Int. Ed.*, 2005, **44**, 5334–5337.
 - M. R. Bermejo, M. Vázquez, J. Sanmartín, A. M. García-Deibe, M. Fondo and C. Lodeiro, *New J. Chem.*, 2002, **26**, 1365–1370.
 - (a) X. Gu and D. Xue, *Inorg. Chem.*, 2006, **45**, 9257–9261; (b) S. Khatua, H. Stoeckli-Evans, T. Harada, R. Kuroda and M. Bhattacharjee, *Inorg. Chem.*, 2006, **45**, 9619–9621.

- 24 A. Kumar, E. Capua, M. K. Kesharwani, Jan M. L. Martin, E. Sitbon, D. H. Waldeck and R. Naaman, *PNAS*, 2017, 2474–2478.
- 25 M. Enamullah, A. Sharmin, M. Hasegawa, T. Hoshi, A.-C. Chamayou and C. Janiak, *Eur. J. Inorg. Chem.*, 2006, 2146–2154.
- 26 C. Janiak, A.-C. Chamayou, A. K. M. Royhan Uddin, M. Uddin, Karl S. Hagen and M. Enamullah, *Dalton Trans.*, 2009, 3698–3709.
- 27 M. Enamullah, A. K. M. Royhan Uddin, G. Pescitelli, R. Berardozi, G. Makhlofi, V. Vasylyeva, A.-C. Chamayou and C. Janiak, *Dalton Trans.*, 2014, 43, 3313–3329.
- 28 M. Enamullah, G. Makhlofi, R. Ahmed, B. A. Joy, M. A. Islam, D. Padula, H. Hunter, G. Pescitelli and C. Janiak, *Inorg. Chem.*, 2016, 55, 6449–6464.
- 29 M. Enamullah, M. A. Quddus, M. R. Hasan, G. Pescitelli, R. Berardozi, G. Makhlofi, V. Vasylyeva and C. Janiak, *Dalton Trans.*, 2016, 45, 667–680.
- 30 I. S. Vasilchenko, A. S. Antsyshkina, D. A. Garnovskii, G. G. Sadikov, M.A. Porai-Koshits, S. G. Sigeikin and A. D. Garnovskii, *Russ. J. Coord. Chem.*, 1994, 20, 824.
- 31 L. Yang, D. R. Powell and R. P. Houser, *Dalton Trans.*, 2007, 955–964.
- 32 H. D. Flack, *Helv. Chim. Acta*, 2003, 86, 905–921.
- 33 A chiral space group needs to have an element from one of the following four pairs of enantiomorphous screw rotations: {31, 32}, {41, 43}, {61, 65}, {62, 64}. Only 22 out of the 230 space groups are chiral. A crystal structure in P21 is chiral but the space group itself is achiral since it does not form one member of an enantiomorphous pair.
- 34 (a) H. D. Flack, *Acta Crystallogr., Sect. A*, 1983, 39, 876–881; (b) H. D. Flack and G. Bernardinelli, *Acta Crystallogr., Sect. A*, 1999, 55, 908–915; (c) H. D. Flack and G. Bernardinelli, *Chirality* 2008, 20, 681–690; (d) H. D. Flack, M. Sadki, A. L. Thompson and D. J. Watkin, *Acta Crystallogr., Sect. A*, 2011, 67, 21–34; (e) H. D. Flack, *Acta Crystallogr. Sect. A*, 2009, 65, 371–389; (f) S. Parsons, H. D. Flack and T. Wagner, *Acta Cryst.*, 2013, B69, 249–259.
- 35 C. Janiak, *J. Chem. Soc. Dalton Trans.* 2000, 3885–3896 and references therein.
- 36 X.-J. Yang, F. Drepper, B. Wu, W.-H. Sun, W. Haehnel and C. Janiak, *Dalton Trans.*, 2005, 256–267 and Supplementary Material therein.
- 37 (a) M. Nishio, *Phys. Chem. Chem. Phys.*, 2011, 13, 13873–13900; (b) M. Nishio, Y. Umezawa, K. Honda, S. Tsuboyama and H. Suezawa, *CrystEngComm*, 2009, 11, 1757–1788; (c) M. Nishio, *CrystEngComm*, 2004, 6, 130–158; (d) C. Janiak, S. Temizdemir, S. Dechert, W. Deck, F. Girgsdies, J. Heinze, M. J. Kolm, T. G. Scharmann and O. M. Zippfel, *Eur. J. Inorg. Chem.*, 2000, 1229–1241; (e) Y. Umezawa, S. Tsuboyama, K. Honda, J. Uzawa and M. Nishio, *Bull. Chem. Soc. Jpn.*, 1998, 71, 1207–1213.
- 38 (a) G. R. Desiraju and T. Steiner, *The weak hydrogen bond*, in: IUCr Monograph on Crystallography, vol. 9, Oxford Science, Oxford, 1999; (b) T. Steiner, *Angew. Chem.*, 2002, 114, 50–80.
- 39 *CrystalExplorer17*, Version 17.5; M. J. Turner, J. J. McKinnon, S. K. Wolff, D. J. Grimwood, P. R. Spackman, D. Jayatilaka and M. A. Spackman, © 2005–217 University of Western Australia, 2017. <http://hirshfeldsurface.net>
- 40 (a) J. J. McKinnon, M. A. Spackman and A. S. Mitchell, *Acta Cryst.*, 2004, B60, 627–668; (b) M. A. Spackman, J. J. McKinnon, *CrystEngComm*, 2002, 4, 378–392; (c) J. J. McKinnon, D. Jayatilaka and M. A. Spackman, *Chem. Commun.*, 2007, 3814–3816.
- 41 J. P. Zhang, Y. Y. Lin, X. C. Huang and X. M. Chen, *Chem. Commun.*, 2005, 1258–1260.
- 42 R.-G. Gonnade, M. M. Bhadbhade and M. S. Shashidhar, *Chem. Commun.*, 2004, 2530–2531.
- 43 X. Ribas, J. C. Dias, J. Morgado, K. Wurst, M. Almeida, T. Parella, J. Veciana and C. Rovira, *Angew. Chem. Int. Ed.*, 2004, 43, 4049–4052; (b) W. Huang and T. Ogawa, *Polyhedron*, 2006, 25, 1379–1385.
- 44 (a) M. Li, Q. Sun, Y. Bai, C. Duan, B. Zhang and Q. Meng, *Dalton Trans.*, 2006, 21, 2572–2578; (b) L. Carlucci, G. Ciani, D. M. Proserpio A. Sironi, *Inorg. Chem.*, 1998, 37, 5941–5943; (c) L. Han and M.-C. Hong, *Inorg. Chem. Commun.*, 2005, 8, 406–419.
- 45 (a) B. Gil-Hernández, J. K. Maclaren, H. A. Höppe, J. Pasan, J. Sanchiz and C. Janiak, *CrystEngComm*, 2012, 14, 2635–2644; (b) M. Wang, J. Y. Li, J. H. Yu, Q. H. Pan, X. W. Song and R. R. Xu, *Inorg. Chem.*, 2005, 44, 4604–4607; (c) C. Kepert, T. Prior and M. J. Rosseinsky, *J. Am. Chem. Soc.*, 2000, 122, 5158–5168; (d) T. Prior and M. J. Rosseinsky, *Inorg. Chem.*, 2003, 42, 1564–1575.
- 46 (a) M. Enamullah, M. A. Quddus, M. M. Rahman and T. E. Burrow, *J. Mol. Struct.*, 2017, 1130, 765–774; (b) M. Enamullah, M. A. Islam, B. A. Joy and G. J. Reiss, *Inorg. Chim. Acta* 2016, 453, 202–209; (c) M. Enamullah, M. A. Islam, B. A. Joy, B. Dittrich, G.J. Reiss and C. Janiak (submitted).
- 47 M. Enamullah, M. A. Quddus, M.A. Halim, M. K. Islam, V. Vasylyeva and C. Janiak, *Inorg. Chim. Acta*, 2015, 427, 103–111.
- 48 M. Enamullah, V. Vasylyeva and C. Janiak, *Inorg. Chim. Acta*, 2013, 408, 109–119.
- 49 A.-C. Chamayou, G. Makhlofi, L. A. Nafie, C. Janiak and S. Lüdeke, *Inorg. Chem.*, 2015, 54, 2193–2203.
- 50 A.-C. Chamayou, S. Lüdeke, V. Brecht, T. B. Freedman, L. A. Nafie and C. Janiak, *Inorg. Chem.*, 2011, 50, 11363–11374.
- 51 APEX2, data collection program for the CCD area-detector system, Version 2.1-0, Bruker Analytical X-ray Systems: Madison (WI), 2006.
- 52 SAINT, data reduction and frame integration program for the CCD area-detector system, Bruker Analytical X-ray Systems: Madison (WI), 2006.
- 53 G. Sheldrick, Program SADABS: Area-detector absorption correction, University of Göttingen, Germany, 1996.
- 54 G. M. Sheldrick, *Acta Crystallogr., Sect. A*, 2008, 64, 112–122.
- 55 K. Brandenburg, Diamond (Version 3.2), Crystal and Molecular Structure Visualization, Crystal Impact – K. Brandenburg & H. Putz Gbr, Bonn (Germany) 2009.
- 56 (a) A. L. Spek, *Acta Crystallogr., Sect. D*, 2009, 65, 148–155; (b) A. L. Spek, PLATON – A multipurpose crystallographic tool, Utrecht University: Utrecht, The Netherlands, 2005.
- 57 C. F. Macrae, I. J. Bruno, J. A. Chisholm, P. R. Edgington, P. McCabe, E. Pidcock, L. Rodriguez-Monge, R. Taylor, J. van de Streek and P. A. Wood, *J. Appl. Cryst.*, 2008, 41, 466–470. Mercury CSD 3.0.
- 58 M. J. Frisch, G. W. Trucks, H. B. Schlegel, G. E. Scuseria, M. A. Robb, J. R. Cheeseman, G. Scalmani, V. Barone, B. Mennucci, G. A. Petersson, H. Nakatsuji, M. Caricato, X. Li, H. P. Hratchian, A. F. Izmaylov, J. Bloino, G. Zheng, J. L. Sonnenberg, M. Hada, M. Ehara, K. Toyota, R. Fukuda, J. Hasegawa, M. Ishida, T. Nakajima, Y. Honda, O. Kitao, H. Nakai, T. Vreven, J. A. Montgomery, Jr., J.E. Peralta, F. Ogliaro, M. Bearpark, J. J. Heyd, E. Brothers, K. N. Kudin, V. N. Staroverov, R. Kobayashi, J. Normand, K. Raghavachari, A. Rendell, J. C. Burant, S. S. Iyengar, J. Tomasi, M. Cossi, N. Rega, J. M. Millam, M. Klene, J. E. Knox, J. B. Cross, V. Bakken, C. Adamo, J. Jaramillo, R. Gomperts, R. E. Stratmann, O. Yazyev, A. J. Austin, R. Cammi, C. Pomelli, J. W. Ochterski, R. L. Martin, K. Morokuma, V. G. Zakrzewski, G. A. Voth, P. Salvador, J. J. Dannenberg, S. Dapprich, A. D. Daniels, Ö. Farkas, J. B. Foresman, J. V. Ortiz, J. Cioslowski and D. J. Fox, *Gaussian 09, Revision C.01*, Wallingford CT, 2009.